Fokker-Planck Modelling of NBI deuterons in ITER

V. Yavorskij 1,2), K. Schoepf 1), V. Goloborod'ko 1,2), M. Cecconello 3,4), L.G. Eriksson 5), M. Khan 1), V. Kiptily 3), A. Korotkov 3), A. Polevoi 6), S. Sharapov 3), S. Reznik 1,2)

1) Institute for Theoretical Physics, University of Innsbruck, Association EURATOM-OEAW, Austria;
2) Institute for Nuclear Research, Ukrainian Academy of Sciences, Kiev, Ukraine
3) EURATOM /UKAEA Fusion Association, Culham Science Centre, Abingdon, Oxfordshire, UK
4) Alfvén Laboratory, Fusion Plasma Physics, Royal Institute of Technology, Stockholm, Sweden
5) Association EURATOM-CEA, CEA/DSM/DRFC, CEA-Cadarache, France
6) ITER Organization, Cadarache, France

e-mail contact of main author: Victor.Yavorskij@uibk.ac.at

Abstract. The paper presents the 3D Fokker-Planck modelling results of the distribution function of energetic deuterons generated in ITER by 1MeV neutral beam injection. For two basic ITER scenarios we calculate the steady-state distributions of beam deuterons in the energy range 100 keV < E < 1 MeV and demonstrate the poloidal profiles of the beam deuteron density, of the NBI generated current as well as of the NBI power deposition to bulk plasma electrons and ions. Further, we evaluate the capability of gamma and NPA diagnostics of NBI ions in ITER.

1. Introduction

Energetic ions generated in ITER by tangential neutral beam injection (NBI) are expected to play a major role in achieving and controlling optimal burning plasma scenarios with external heating and/or current drive [1]. The investigation of NBI impact on specific processes in tokamak plasmas requires detailed information about the distribution function of beam ions, which is strongly anisotropic in velocity space and inhomogeneous in spatial coordinates (e.g. [2-4]). In order to identify the crucial points in the beam physics and to assess the diagnostic tools capable of measuring NBI-produced ions with good accuracy we present here results of Fokker-Planck modelling of the deuteron distribution function produced in ITER by 1MeV NBI and model gamma-ray and NPA diagnostic techniques previously used on JET [2]. Considered are the distributions of beam deuterons in the energy range 100 keV < E < 1 MeV for ITER Scenario 2 (standard H-mode, I/B=15MA/5.3T) and for Scenario 4 (steady-state, I/B=9MA/5.3T) [5]. For these two scenarios Fig. 1 compares the respective radial profiles of the safety factor and of the Spitzer slowing down time of 1 MeV deuterons. A steady-state distribution formed by a constant NBI source during the slowing time of a 1MeV deuteron is mostly investigated, though – for evaluating the capability of gamma diagnostics of fast ions [6] in ITER – the relaxation of the beam deuteron distribution functions after NBI switch-off is

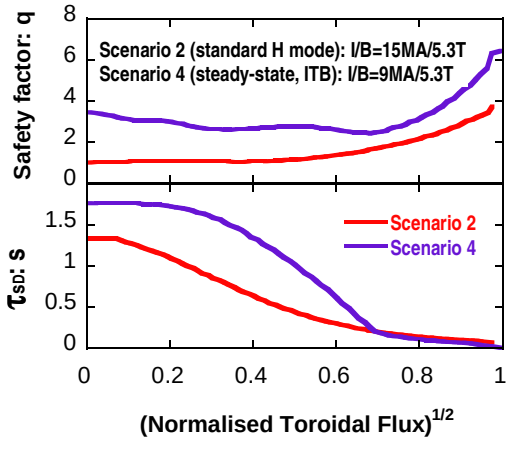

Fig. 1: Radial profiles of safety factor and of deuteron Spitzer slowing down time, τ_{sD}, in ITER scenario 2 and 4 [5].

examined as well. Referring to the specific NBI injection geometry of ITER and considering finite beam thickness and divergence, the source of NBI generated deuterons is calculated as a 4-dimensional distribution function in real space [4]. Based on this source the steady-state deuteron distributions are computed using the 3D in constants-of-motion (COM) Fokker-Planck code, which was earlier tested in interpretive modelling of beam ions in JET Trace Tritium Experiments (TTE) [2]. For the present calculations this 3D Fokker-Planck model has been extended to take into account the beam divergence, which is important to obtain a higher spatial resolution of the NBI ion distribution function [4].

2. Modelling results

Based on the calculated 3D COM distribution functions of beam deuterons in ITER we model the poloidal profiles of the density of energetic deuterons, of the NBI power deposition to bulk plasma electrons and ions as well as of the NBI generated current. Similar to our simulations in [7, 8] the (*R*,*Z*)-profiles of gamma-emission from nuclear reactions of beam deuterons with plasma impurities are also modelled as well as the energy spectra of neutral deuterium (D^0) fluxes induced by beam deuterons. For examining the time evolution and relaxation of the deuteron distribution function after NBI switch-off we employ a time-dependent Fokker-Planck approach that was used for the analysis of the evolution of alpha particle induced gamma-emission in JET TTE [9, 10].

a) Distribution function of NBI deuterons

Figure 2 compares the COM deuteron distributions generated by 16.5MW on-axis (left) and 16.5MW off-axis (right) NBI in the steady state ITER scenario in the case of standard beam divergence [4]. The red lines in Fig. 2 represent deuterons produced from

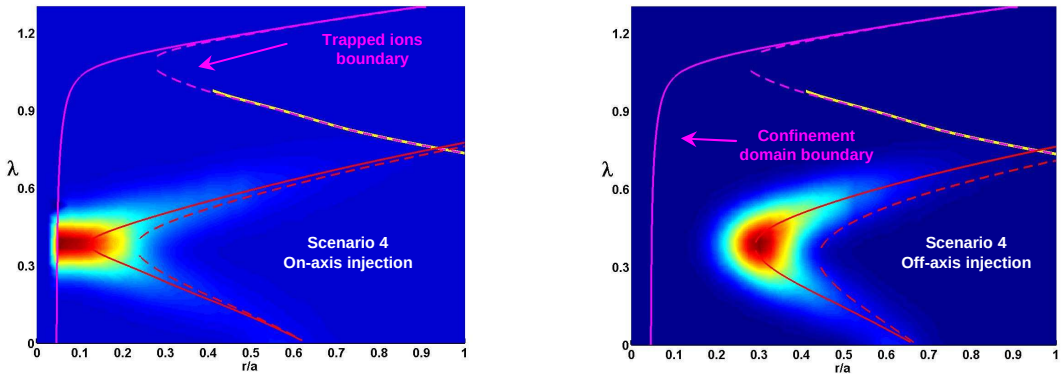

Fig. 2: Contours of the 3D COM distribution function of 1MeV beam deuterons in the plane spanned by the normalized magnetic moment $\lambda=\mu B/E$ and the maximum radial orbit coordinate for 16.5MW on-axis and 16.5MW off-axis NBI in ITER scenario 4 (ITB). Red lines denote the beam axis and violet ones show the boundary of the confinement domain of co-going particles (solid lines) and that of toroidally trapped particles (broken lines). The yellow line corresponds to the separatrix between trapped and circulating particles.

neutrals in the vicinity of the beam axis (solid and broken lines correspond to the beam path before and, respectively, after the tangency point, R_t=5.28m). The majority of beam ions at E=1MeV appears as well-circulating core-localised (r_{max}/a < 0.3-0.4) particles with a

normalized magnetic moment $\lambda \sim 0.4$ ($V_{||}/V$~0.7-0.8). Clearly seen is the effect of NBI direction on the radial profile of 1 MeV beam deuterons. In Fig. 3 we display the modelled profiles of the density of energetic NBI deuterons (100keV < *E* < 1MeV) in the (*R*, *Z*)-plane for the 4thscenario. While the RHS image shows the poloidal density profile of fast deuterons

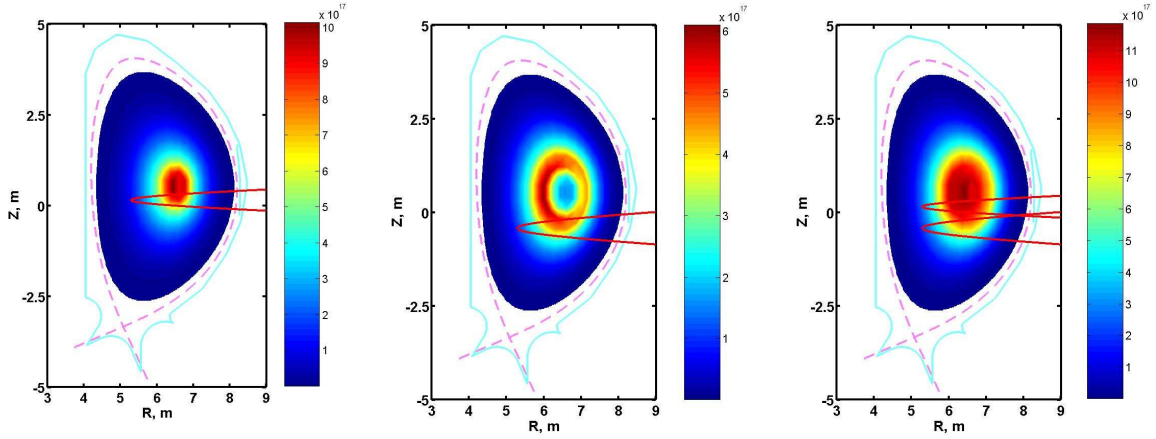

Fig. 3: Modelled profiles of the density (m^{-3}) of NBI deuterons (100keV<E<1MeV) in Scenario 4 for 16.5MW on-axis (left), 16.5MW off-axis (center) and (16.5MW on-axis +16.5MW off-axis) 1MeV D^0- NBI (right).

generated by two 1MeV D^0 beams with 33MW total NBI power (16.5MW on-axis + 16.5MW off-axis), the two images on the left and in the center illustrate the partial densities from 16.5MW on-axis and 16.5MW off-axis injection, respectively. An essential poloidal asymmetry of the density of beam ions becomes apparent, which is most pronounced in the case of off-axis injection. Figure 4 displays the calculated density profiles of NBI deuterons and of fusion alphas in the plasma mid-plane for scenario 4. The red curve represents our modelled profile of the beam deuteron density, which is seen to reasonably agree with the ASTRA simulation in [5] (blue curve). The maximum density of beam deuterons in this scenario is ~10^{18} m^{-3} and amounts to about 25% of the maximum density of fusion alphas [11].

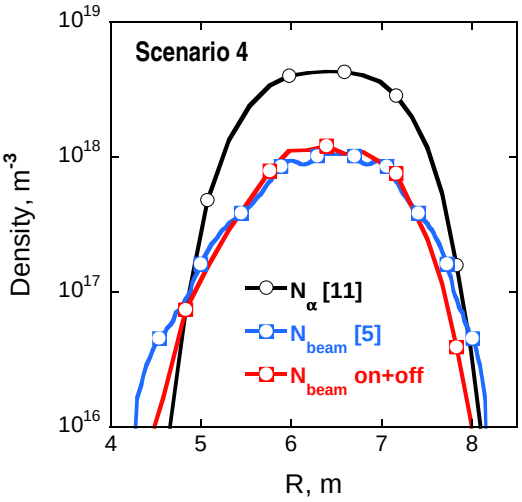

Fig. 4: Mid-plane profiles of the modelled density of NBI *deuterons (100keV < E < 1MeV)* for *the 4th ITER scenario. The black curve represents the mid-plane profile of fusion alphas modelled in [11].*

b) Current driven by beam deuterons

Due to the strong anisotropy of beam ions in longitudinal velocity (majority of them are co-circulating) a significant contribution of beam deuterons to the plasma current can be expected. This is confirmed by Fig. 5 that compares, for the 2nd and 4th ITER scenario, the

mid-plane densities of the beam driven current $j_{beam}(R, Z=Z_{ax})$, of the total plasma current $j_{tot}(R, Z=Z_{ax})$ [5] and of the current $j_{\alpha}(R, Z=Z_{ax})$ induced by fusion alphas [11]. It is seen that the current driven by beam deuterons will constitute a substantial part of the plasma current and in the case of Scenario 4 can be even comparable with j_{tot} [5] and the alpha driven current j_{α}. Thus NBI deuterons, by analogy with fusion alphas [11], can noticeably affect the

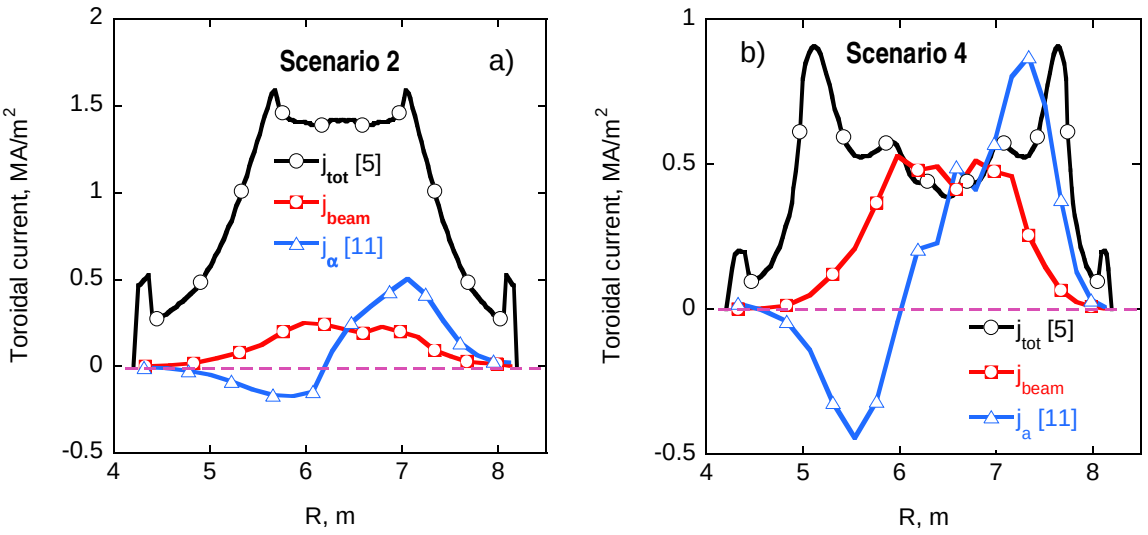

Fig. 5: Mid-plane profiles of the modelled densities of currents driven by beam deuterons, j_{beam}, and by fusion alphas, j_{α}, for the 2nd (a) and 4th (b) ITER scenario

plasma equilibrium in ITER, at least in the case of the reversed shear plasma in Scenario 4. Note that the total beam driven current $j_{b\,tot}$, must include that of beam ions and the electron reversed current and can be represented as $j_{b\,tot} = \langle j_b \rangle \left[1 - Z_b (1-g)/Z_{eff}\right]$, where $g \sim (r/R)^{1/2}$ stands for the trapped electron correction to $j_{b\,tot}$ [12].

c) NBI power deposited to the bulk electrons and ions

The important impact of NBI on bulk plasma components is due to the respective

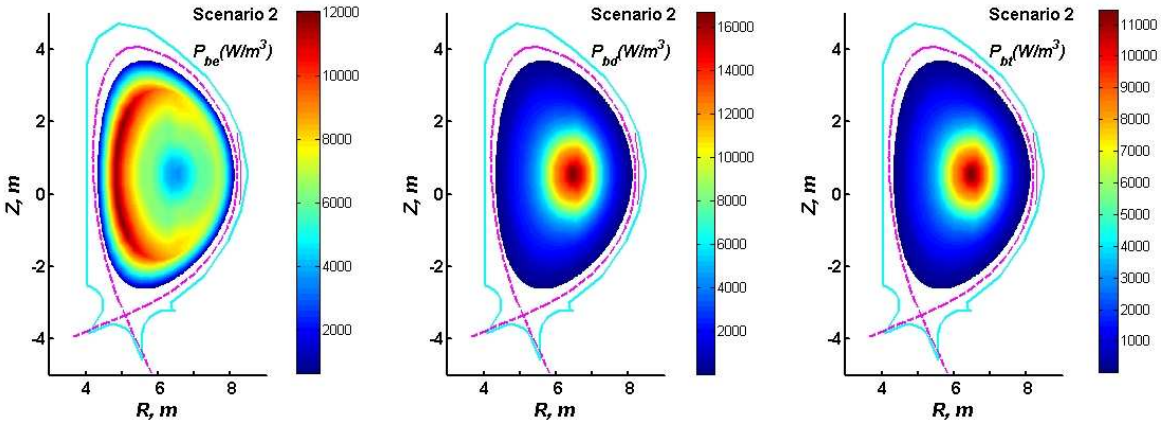

Fig. 6: Modelled R,Z profiles of the density of NBI power (Wm^{-3}) deposited to the bulk electrons (left), deuterons (center) and tritons (right) in Scenario 2.

deposition profiles of injection power to plasma electrons and ions. In Fig. 6 we illustrate for the 2nd ITER scenario the modelled *R,Z* distributions of the density of NBI power allocated to plasma electrons, P_{be}, to bulk deuterons, P_{bd}, and to tritons, P_{bt}. The NBI power deposition to plasma electrons is characterized by a hollow profile with the maximum $P_{be} > 0.01\text{MW/m}^3$ occurring at the high-*B* side of the plasma ($R \sim 5$m). This enhanced P_{be} at the plasma periphery is due to a relatively high slowing down frequency of beam deuterons on the electrons $\upsilon_s^{D/e} \sim 1/\tau_{sD}$ at the plasma edge (see Fig. 1). Note that, in contrast to P_{be}, the NBI powers transferred to plasma deuterons, P_{bd}, and tritons, P_{bt}, are localized in the plasma core in accordance with the *R,Z* distribution of slowing down rates of beam deuterons on bulk ions, $\upsilon_s^{D/i} \sim n_i$, which peak in the plasma center. Interestingly, for the 2nd scenario the maximum value of the density of NBI power deposited to bulk deuterons, P_{bd} , is nearly 0.02MW/m^3, while the maximum of P_{bt} is of the order of 0.01MW/m^3. Similar features of NBI power allocations to the bulk plasma components are observed also for scenario 4 as shown in Fig. 7. However, in this scenario, the hollow shape of P_{be} is less pronounced with a maximum of P_{be} below 0.01MW/m^3. Further, the maximum values of the density of NBI power depositions to bulk deuterons and tritons in the 4th scenario exceed those in the 2nd scenario by about 40%.

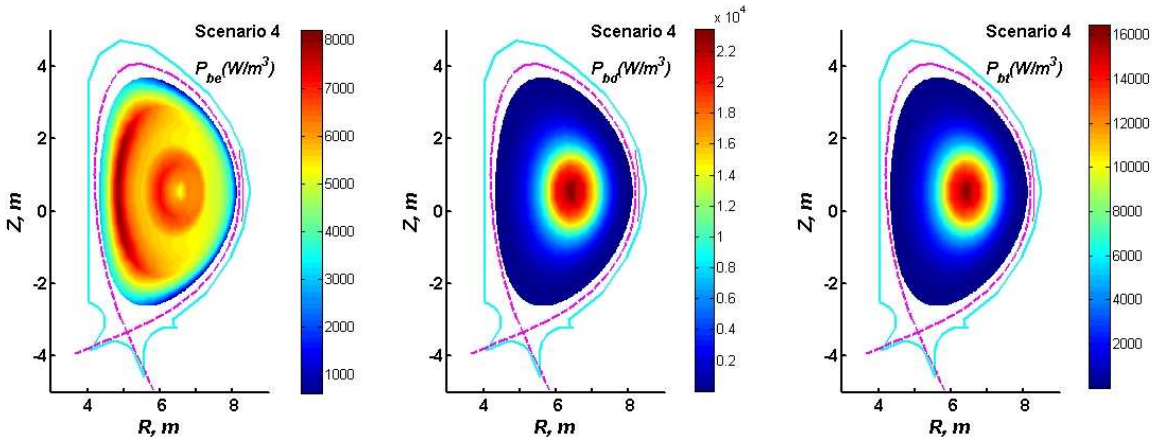

Fig. 7: Modelled R,Z profiles of the density of NBI power (Wm^{-3}) deposited to the bulk electrons (left), deuterons (center) and tritons (right) in Scenario 4.

d) Gamma-emission and neutral particle fluxes induced by NBI ions

The knowledge of the beam ion distribution function in 3D COM space allows for determination of both the (*R, Z*)-profiles as well as the temporal evolution of rates of gamma-emission from nuclear reactions of beam deuterons with Be and C impurities [6, 9], which are viewed important for gamma diagnostics of NBI ions in ITER [13]. Thus the spatial (*R,Z*)- distributions of beam deuterons can be well reproduced from the profiles of the emission rates of γ-radiation produced in reactions of energetic deuterons with plasma impurities. This is demonstrated by Fig. 8 representing the Fokker-Planck calculations of 3.09 MeV γ-emission rates due to $^{12}\text{C}(d, p\gamma)^{13}\text{C}$ interactions of beam ions and 2.5% carbon impurities. It is seen that, in the steady state scenario, the maximum gamma-emission rate R_γ amounts to higher values than in scenario 2 and also features a flatter distribution $R_\gamma(R,Z)$ in the core region. This sensitivity of NBI deuteron induced γ-emission profiles to the

operational scenario, which is nearly independent of the type of gamma emitting reaction, makes multi-channel gamma measurements a viable tool for diagnostics of NBI generated ions. On the other hand, examining the time evolution of gamma-emission induced by NBI

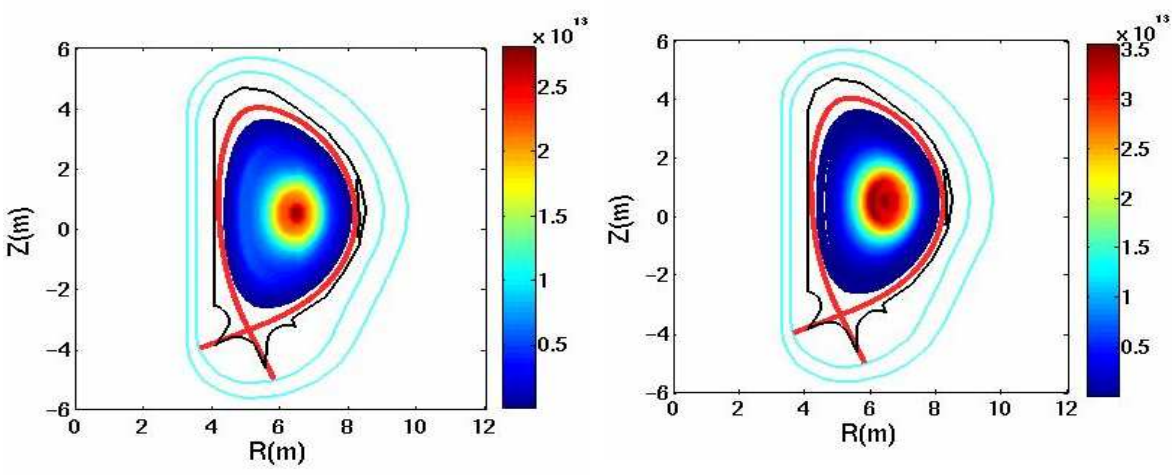

Fig. 8: Modelled profiles of 3.09MeV γ-emission rates from $^{12}C(d,p\gamma)^{13}C$ reactions in $m^{-3}s^{-1}$ in the case of superposition of 16.5MW on-axis and 16.5MW off-axis injection for the 2nd scenario (left) and the 4th scenario (right).

deuterons can give us information about slowing down and loss rates of beam ions. The capability of such gamma diagnostics of beam ions can be illustrated by a qualitative analysis of R_γ based on a 1D Fokker-Plank model [9]

$$R_\gamma(t) \propto \int_{E_{\min}}^{\infty} dE\sqrt{E} \int_0^{\tau_{D\gamma}} d\tau\, \sigma_\gamma(E')\sqrt{E'} \exp\left(-\frac{\tau}{\tau_l}\right) S(E, t-\tau) \tag{1}$$

with

$$E' = \left[E^{3/2} \exp\left(-\frac{3\tau}{\tau_{sD}}\right) - E_c^{3/2}\left(1-\exp\left(-\frac{3\tau}{\tau_{sD}}\right)\right)\right]^{2/3}, \quad \tau_{D\gamma} = \frac{\tau_{sD}}{3} \ln \frac{E^{3/2}+E_c^{3/2}}{E_{\min}^{3/2}+E_c^{3/2}}, \tag{2}$$

where $S(E,t)$ is the time-dependent source term of NBI ions, σ_γ specifies the cross section of the considered nuclear reaction of deuterons with impurity ions, $E_{\min}$ denotes the energy threshold for this reaction, τ_l the average loss time and $E_c \sim 20T_e$ the critical energy [14]. Taking $S(E,t) \sim \delta(E\text{-}E_0)\eta(\text{-}t)$, where $\delta(x)$ designates the Dirac delta function and $\eta(x)$ the Heaviside step function, we obtain from Eq. (1) the following expression describing the temporal evolution of R_γ after NBI has been switched off at t=0:

$$R_\gamma(t>0) \propto \sqrt{E} \int_t^{\tau_{D\gamma}} d\tau\, \sigma_\gamma(E')\sqrt{E'} \exp\left(-\frac{\tau}{\tau_l}\right)\Bigg|_{E=E_0}, \quad E_0 = 1\ \text{MeV}. \tag{3}$$

Figure 9 demonstrates such an evolution of gamma emission produced by $^9Be(d,n\gamma)^{10}B$ interactions of beam deuterons and beryllium impurities after NBI switch-off. The gamma

emission rates are seen to decay faster when the critical energy of deuterium ions is higher and their confinement is degraded. In the case of well confined beam deuterons the characteristic time of R_γ-decay is about $0.2\tau_{sD}$ at low E_c=100 keV and decreases to ~ $0.1\tau_{sD}$ at E_c=500 keV. Poor confinement associated with $\tau_l < 0.1\tau_{sD}$ will significantly enhance the decay rates of gamma emission. Thus we conclude that for the experimental assessment of the slowing-down and/or loss rates of the beam deuterons the gamma measurements with about 50*ms* time resolution are required.

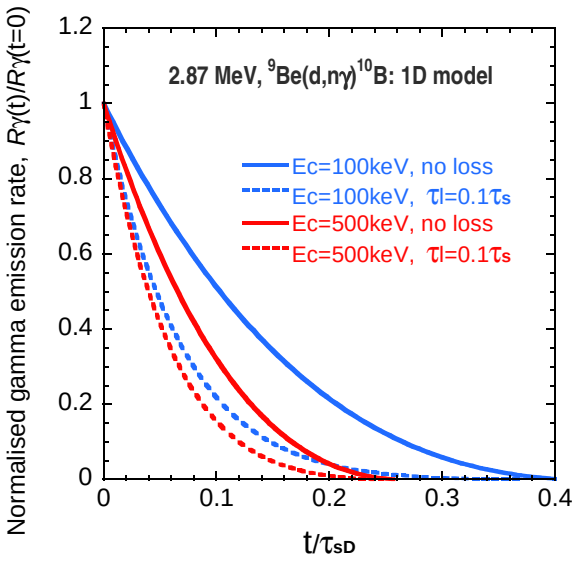

Fig. 9: Evolution of 2.87 MeV gamma emission from nuclear reactions of beam deuterons with 2,5% beryllium impurities after NBI switch-off.

An examination of the confinement of NBI ions in ITER plasmas may be undertaken also by analyzing energetic neutral particle fluxes emitted from the plasma, which are mainly formed by recombination and charge exchange reactions of NBI generated deuterons. Knowledge of the distribution functions of beam ions in 3D COM space as well as of the bulk electrons and background neutrals allows to simulate the energy spectra of D^0 neutrals produced by NBI deuterons. The modeling carried out demonstrated a prominent sensitivity of these spectra to the plasma scenario chosen and confirms the capability of NPA diagnostics of NBI ions in ITER.

3. Summary

Our Fokker-Planck modelling of NBI deuterons in ITER makes evident the sensitivity of the spatial and velocity distributions of NBI generated ions to different operation scenarios. NBI deuterons are shown to be strongly anisotropic over their longitudinal energy resulting in a substantial beam driven current. In the steady-state scenario this NBI induced current is, in the core region, even comparable to the total plasma current. The poloidal profiles of the density of beam deuterons as well as of the NBI power deposition to electrons and to bulk plasma ions are calculated. The simulations performed demonstrate the potential of NBI ion diagnostics in ITER via measurements of gamma-emission from nuclear reactions of fast ions with Be and C impurities, and also via neutral particle detectors analyzing the fluxes of energetic deuterium neutrals launched from the plasma.

Acknowledgement

This work, supported by the European Communities under the contract of Association between EURATOM/ÖAW was carried out within the framework of the European Fusion Development Agreement (particularly within the TW6-TPDS-DIADEV project). The views and opinions expressed herein do not necessarily reflect those of the European Commission.

References

[1] FASOLI, A., et al., Nucl. Fusion **47** (2007) S264–S284.
[2] HAWKES, N., et al., Plasma Phys. Control. Fusion **47** (2005) 1475.
[3] EGEDAL, J., et al., Nucl. Fusion **45** (2005) 191.
[4] YAVORSKIJ, V., et al., 10th IAEA TM on Energetic Particles, Kloster Seeon, Germany, O-11 (2007).
[5] POLEVOI, A.P., et al., J. Plasma Fusion Res. Series **5** (2002) 82.
[6] KIPTILY, V.G., et al., Phys. Rev. Lett. **93** (2004) 115001.
[7] YAVORSKIJ, V., et al., 34th EPS Plasma Physics Conference, Warsaw, Poland, P2.041 (2007).
[8] GOLOBOROD'KO, V., et al., 10th IAEA TM on Energetic Particles, Kloster Seeon, Germany, P11 (2007).
[9] YAVORSKIJ, V., et al., 20th IAEA Fusion Energy Conference, Vilamoura, Portugal, TH/P4-4 (2004).
[10] STORK, D., et al., Nucl. Fusion **45** (2005) S181.
[11] YAVORSKIJ, V., et al., 35th EPS Plasma Physics Conference, Crete, P1.087 (2008).
[12] HIRSHMAN, S.P., Phys. Fluids **31**, (1988) 3150.
[13] KIPTILY, V.G., et al., "Fast ion JET diagnostics: confinement and losses", in Burning Plasma Diagnostics, editors P.Orsitto, G. Gorini, E. Sindoni, M. Tardocci, AIP Conference proceedings, Varenna, Italy (2007) p 283.
[14] FIORE, C.L., et al., Nucl. Fusion **28** (1988) 1315.